acid anodized specimen (control specimen) are also given in Figure 4.44. The crack growth behavior for CAA Ti-6Al-4V specimens that had been bonded and then thermally treated **(bond/heat)** at 371°C in air for selected times and then immersed in boiling water are shown in Figure 4.45. The crack length results for as-bonded (no thermal treatment) chromic acid anodized specimen (control specimen) are also given in Figure 4.45. The crack growth curves indicate no difference in durability after 5000 hours of immersion in boiling water when comparing the results for as-bonded (no thermal treatment) control specimens and heat/bond specimens. The durability performance in boiling water for wedge specimens that were bonded and then thermally treated at 371°C in air for 0.5 and 1.0 hour was comparable to that for as-bonded control specimens. However, it is noteworthy that the specimens that were bonded and then heated at 371°C in air for 3 hours failed completely (debonded) upon insertion of the wedge, and therefore were not tested in boiling water. In Figure 4.44 a single data point is located at zero time and at about 92 mm to represent this behavior.

A visual examination of debonded specimens shows crack propagation within the adhesive (cohesive failure) during the entire test period (>5000 hours) for as-bonded and heat/bond specimens. The bond/heat specimens that were thermally treated at 371°C in air for 0.5 and 1.0 hour also show cohesive failure within the adhesive during the entire test period. Visual examination of failure surfaces for debonded specimens that were bonded and then thermally treated (bond/heat) at 371°C in air for 3.0 hours indicated that failure (crack propagation) was definitely not in the adhesive; the two failure surfaces from each specimen had a glossy metal like appearance which suggest that the locus of failure is at the metal/oxide interface. However, as discussed later, the SEM and XPS surface analyses of failure surfaces of bond/heat specimens (371°C for 3 hours in air) revealed that failure is primarily within the anodic oxide coating.

The strain energy release rate versus immersion time plots for as-bonded (non-treated) and heat/bond specimens are given in Figure 4.46. The strain energy release rate versus immersion time plots for as-bonded (non-treated) and bond/heat specimens are given in Figure 4.47. As discussed in chapter 1, the strain energy release rate (G) is characteristic of the medium in which

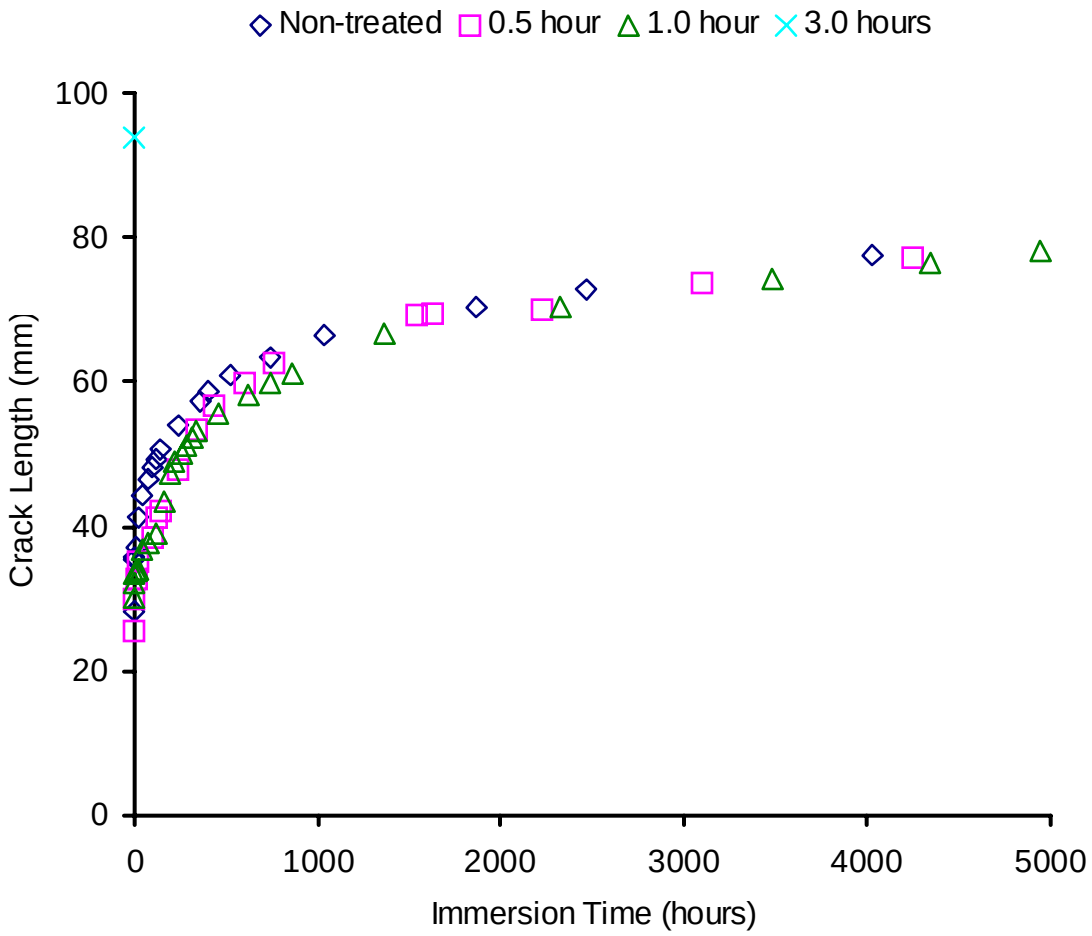

Figure 4.45. Wedge test crack length vs. immersion time in boiling water for CAA Ti-6Al-4V bonded with FM-5 adhesive for non-thermally treated (◊) and for CAA Ti-6Al-4V alloy bonded and then thermally treated at 371°C for 0.5 hr ( ), 1.0 hr (Δ) and 3.0 hrs (×) in air.

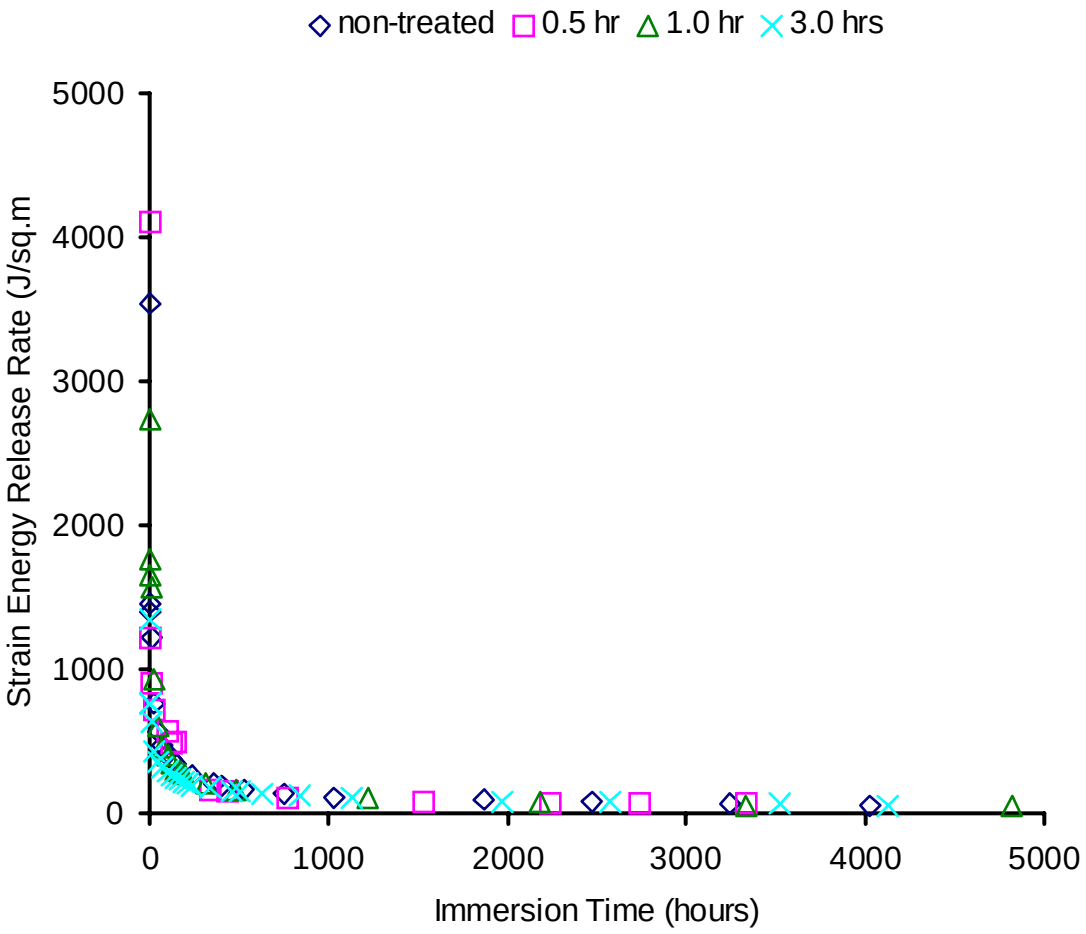

Figure 4.46. Strain energy release rate vs. immersion time in boiling water for CAA Ti-6Al-4V bonded with FM-5 adhesive for non-thermally treated (◊) and for CAA Ti-6Al-4V alloy thermally treated at 371°C for 0.5 hr ( ), 1.0 hr (Δ) and 3.0 hrs (×) in air and then bonded.

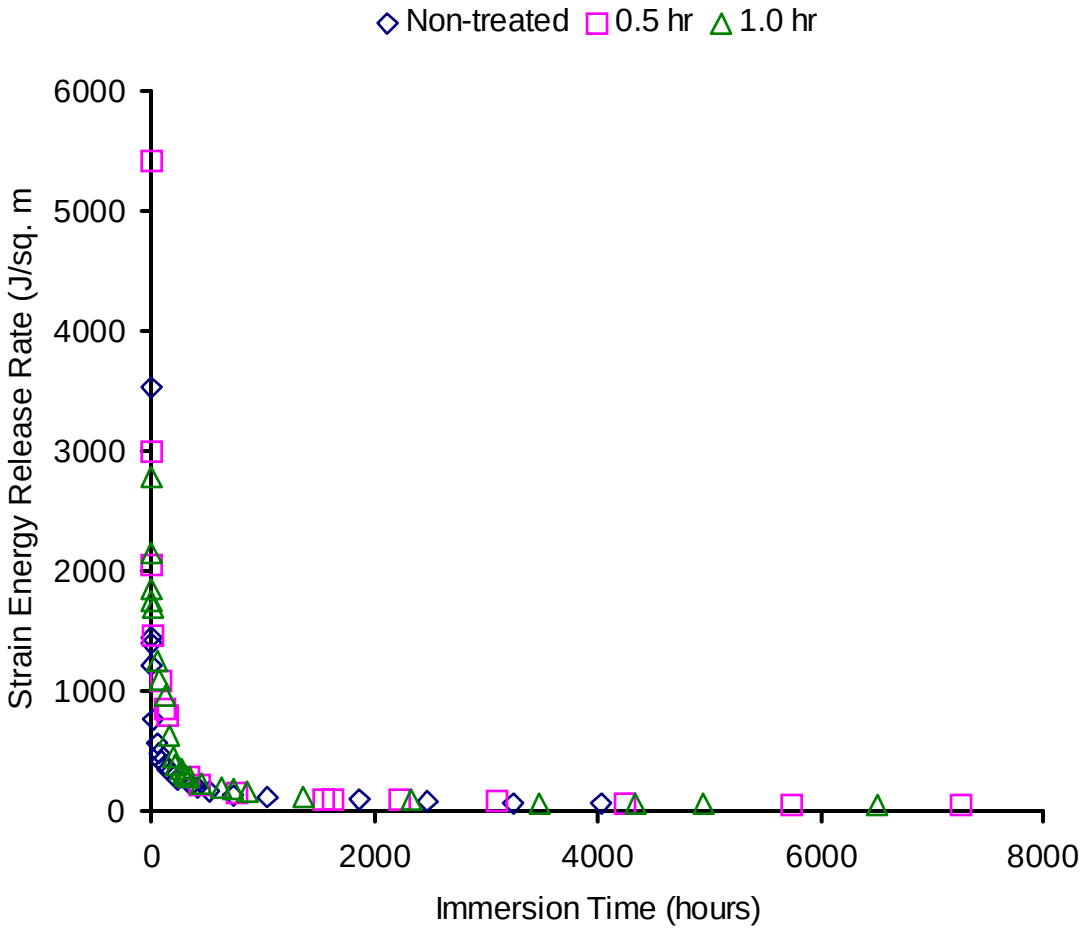

Figure 4.47. Strain energy release rate vs. immersion time in boiling water for CAA Ti-6Al-4V bonded with FM-5 adhesive for non-thermally treated (◊) and for CAA Ti-6Al-4V alloy bonded and then thermally treated at 371°C for 0.5 hr ( ) and 1.0 hr (Δ) in air.

the crack propagates. Therefore, any differences in the strain energy release rate among the wedge specimens with various thermal treatment histories would indicate that the adhesive has undergone physical and/or chemical aging. However, no significant differences in strain energy release rate were noted for wedge specimens immersed in boiling water with various thermal treatment histories. The average strain energy release rate decreased rapidly to about 90% of its initial value in about 192 hours after the specimens were immersed in boiling water, and thereafter it continued to decrease, though at a much slower rate. After about 5000 hours in boiling water, the average strain energy release rate for as-bonded, bond/heat and heat/bond specimens was about 60 J/m^2. It is expected that the crack tends to continue to propagate within the adhesive until an equilibrium is reached when strain energy release rate (G_{arrest}) is equal to the resistance to fracture of the adhesive.

As discussed later, FTIR characterization and XPS analyses of failure surfaces of the wedge specimens suggest that no detectable chemical degradation (via hydrolysis) of the FM-5 adhesive occurs in boiling water. The wedge test data together with XPS and FTIR test results suggest that a combination of mechanical stress (wedge-load) and water induced plasticization of the FM-5 adhesive at the crack tip are likely responsible for the loss of adhesive strength in boiling water. In general, all organic adhesives absorb water to some extent and the mechanical behavior of adhesives is changed due to physical and/or chemical interactions of the adhesive with the ingressing water molecules [122, 123]. The physical changes affect molecular motions, mobility, relaxations, dynamics, etc. The effect of water on molecular mobility and relaxations in the glassy state (physical aspect) is instantaneous. The chemical interactions with water include hydrolysis, hydrogen-bonded complexes, etc. Most of the modern structural polyimide adhesives are resistant to hydrolysis in neutral water (pH ≈ 7.0), however, physical interaction in the form of plasticization is common. The pH of de-ionized boiling water used for immersion wedge tests in the present work was always near neutral range (pH = 6-7, tested with pH paper) during the entire test period.

4.3.2.2 Surface Characterization of Failure Surfaces by SEM

The SEM photomicrographs for failure surfaces of a representative **as-bonded** (no heat treatment) wedge specimen that was immersed in boiling water for 144 hours are shown in Figure 4.48. The two failure sides of the same specimen are arbitrarily labeled as "side A" and "side B". The SEM photomicrographs of failure surfaces of a non-treated specimen revealed weave-type features which are characteristic of the pattern of the woven glass scrim cloth in the adhesive.

The SEM photomicrographs of failure surfaces of representative **heat/bond** wedge specimens that were prepared by thermal treatment at 371°C in air for 0.5, 1.0 and 3.0 hrs, respectively, and bonded, and then immersed in boiling water for 144 hours are shown in Figures 4.49 – 4.51. The weave-type features are also observed on failure surfaces (side A and side B) of heat/bond specimens.

The SEM photomicrographs of representative **bond/heat** wedge specimens that were bonded and then thermally treated at 371°C in air for 0.5 hr and 1.0 hr respectively, and then immersed in boiling water for 144 hours also showed weave-type pattern on the failure surfaces, see Figures 4.52 and 4.53. The presence of such weave-type patterns on both sides (side A and side B) of the same sample indicates that failure occurred within the adhesive. For bond/heat specimens that were bonded and then thermally treated at 371°C for 3 hours in air, the SEM photomicrographs show the imprints of the adhesive, but the weave-type pattern is not observed on the failure surfaces (see Figure 4.54). The relatively smooth features in the SEM photomicrographs for bond/heat failure surfaces, that were thermally treated at 371°C for 3 hours in air, are consistent with the XPS results, in that failure occurs within the oxide. A thin layer of oxide covers the adhesive on the side A failure surface and the imprint of the scrim cloth is evident on the side B failure surface.

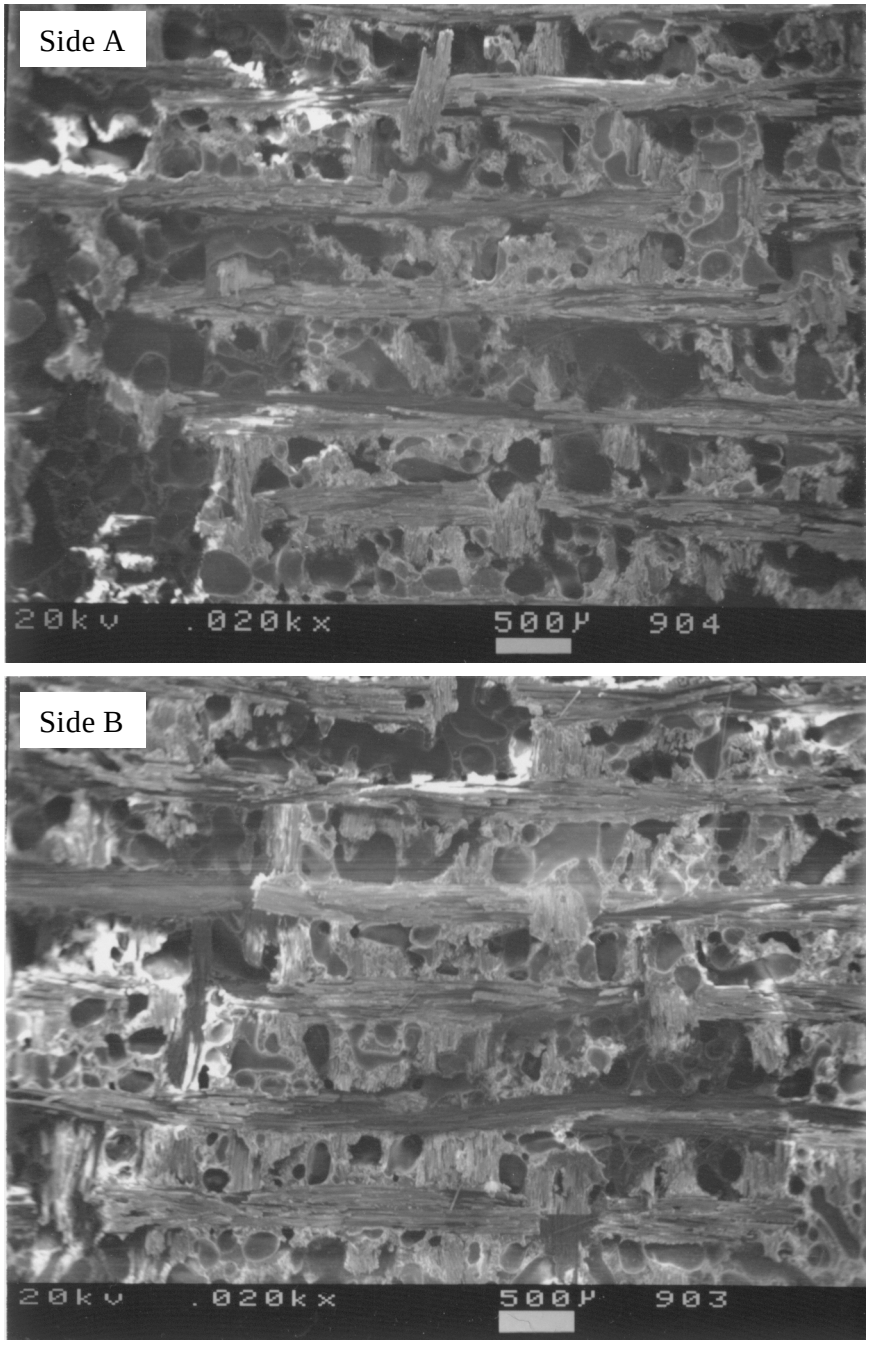

Figure 4.48. SEM photomicrographs of failure surfaces of a representative as-bonded specimen (no heat treatment) that was immersed in boiling water for 144 hrs. The SEM photomicrographs of the two failure surfaces are not necessarily for corresponding spots.

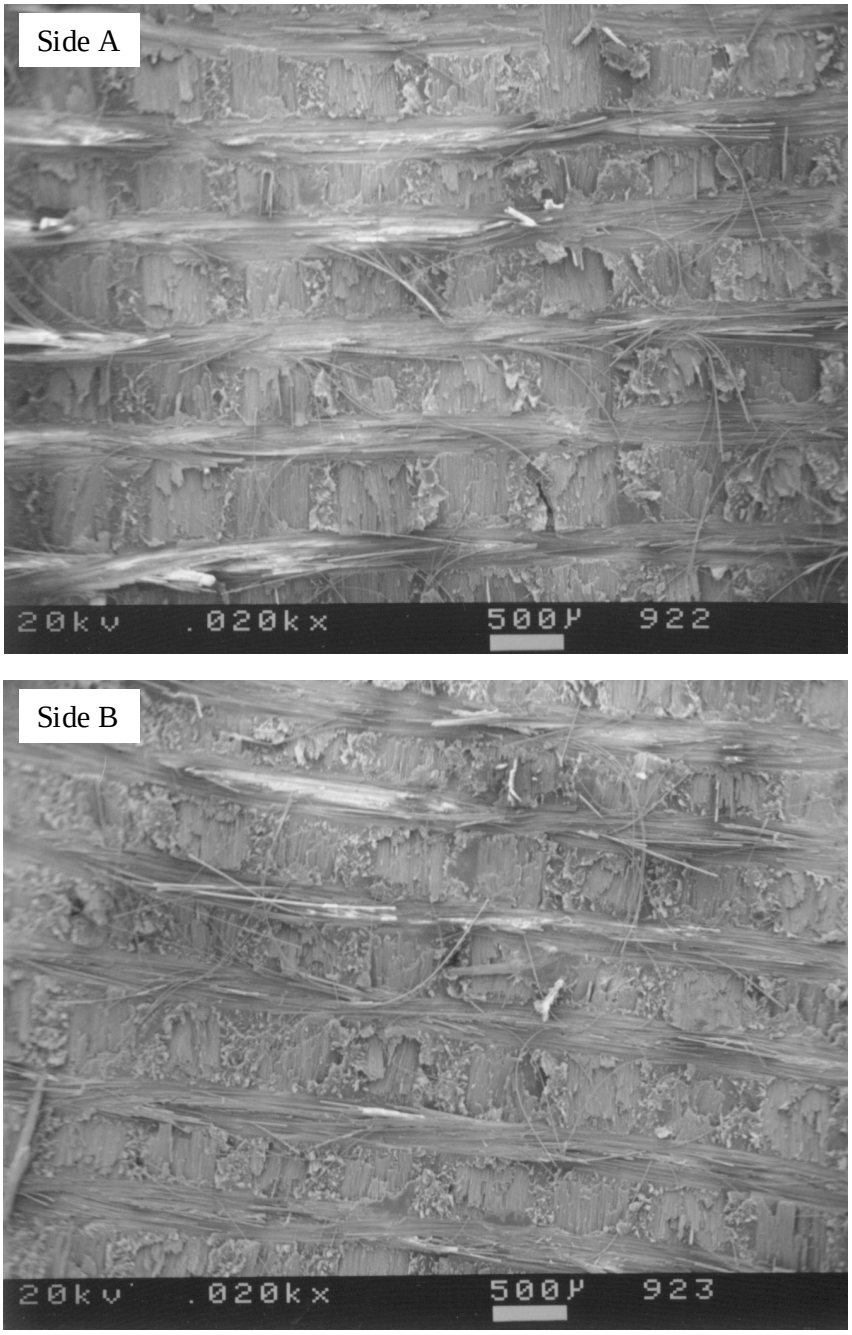

Figure 4.49. SEM photomicrographs of failure surfaces of a representative wedge specimen that was thermally-treated at 371°C for 0.5 hours in air and then bonded (heat/bond) and immersed in boiling water for 144 hrs. The SEM photomicrographs of the two failure surfaces are not necessarily for corresponding spots.

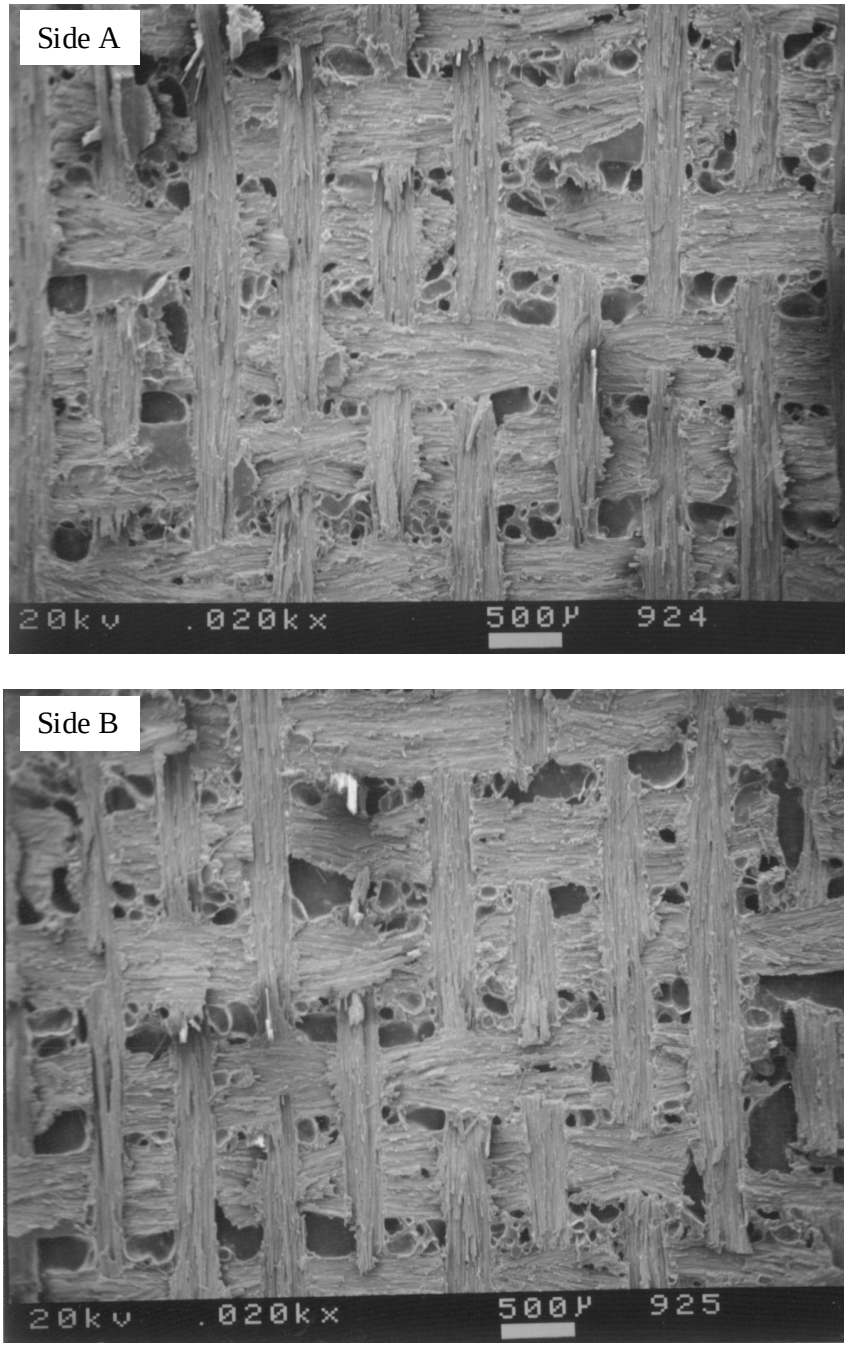

Figure 4.50. SEM photomicrographs of failure surfaces of a representative wedge specimen that was thermally-treated at 371°C for 1.0 hour in air and then bonded (heat/bond) and immersed in boiling water for 144 hrs. The SEM photomicrographs of the two failure surfaces are not necessarily for corresponding spots.

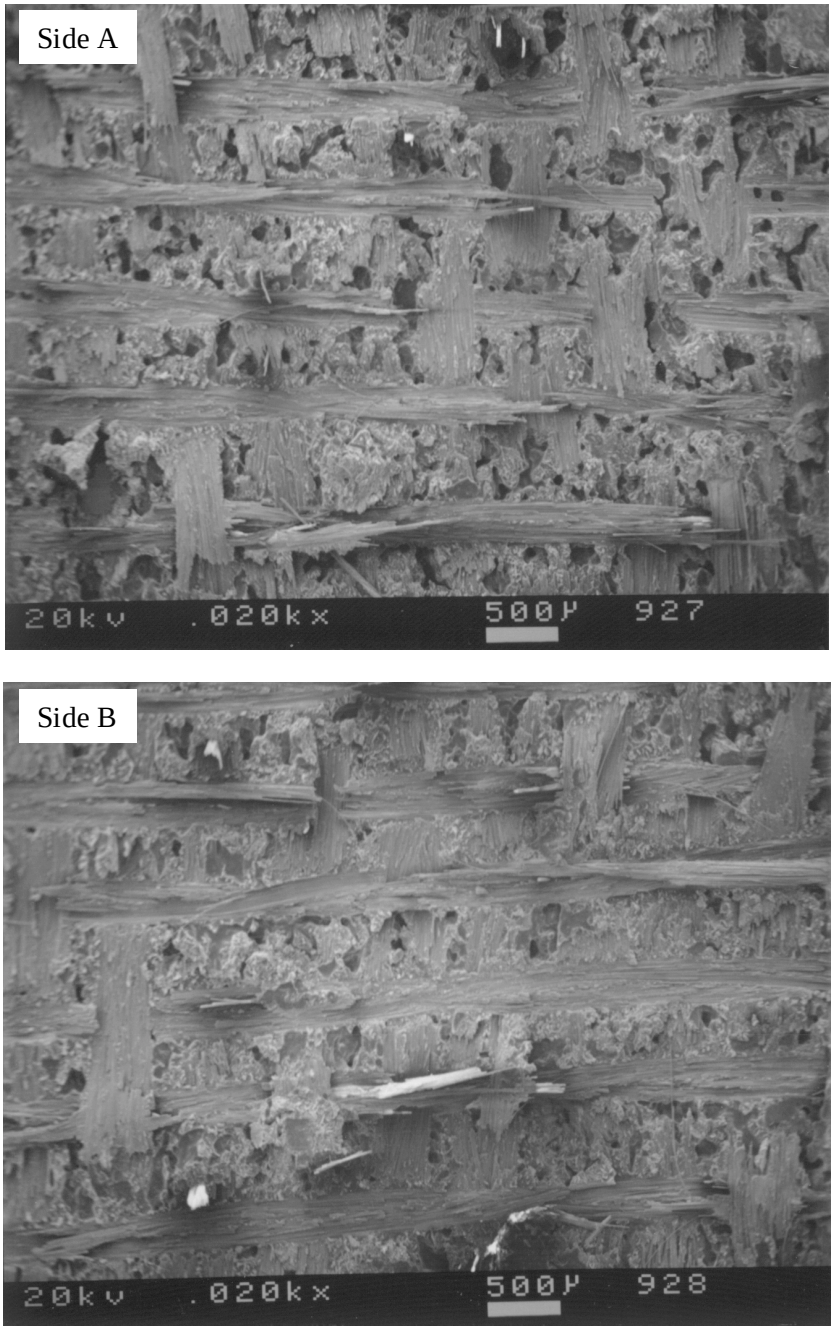

Figure 4.51. SEM photomicrographs of failure surfaces of a representative wedge specimen that was thermally-treated at 371°C for 3.0 hours in air and then bonded (heat/bond) and immersed in boiling water for 144 hrs. The SEM photomicrographs of the two failure surfaces are not necessarily for corresponding spots.

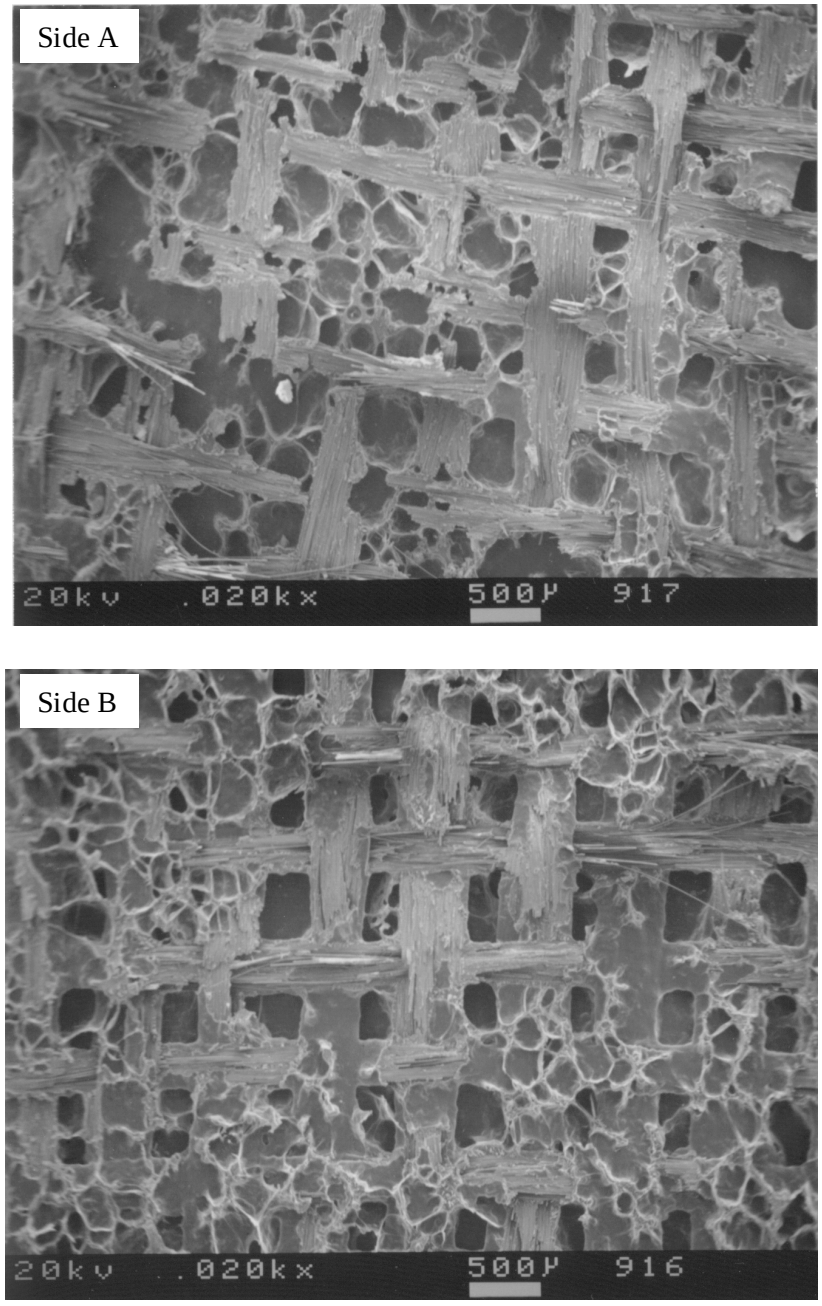

Figure 4.52. SEM photomicrographs of failure surfaces of a representative wedge specimen that was bonded and then thermally treated at 371°C for 0.5 hour in air (bond/heat) and immersed in boiling water for 144 hrs. The SEM photomicrographs of the two failure surfaces are not necessarily for corresponding spots.

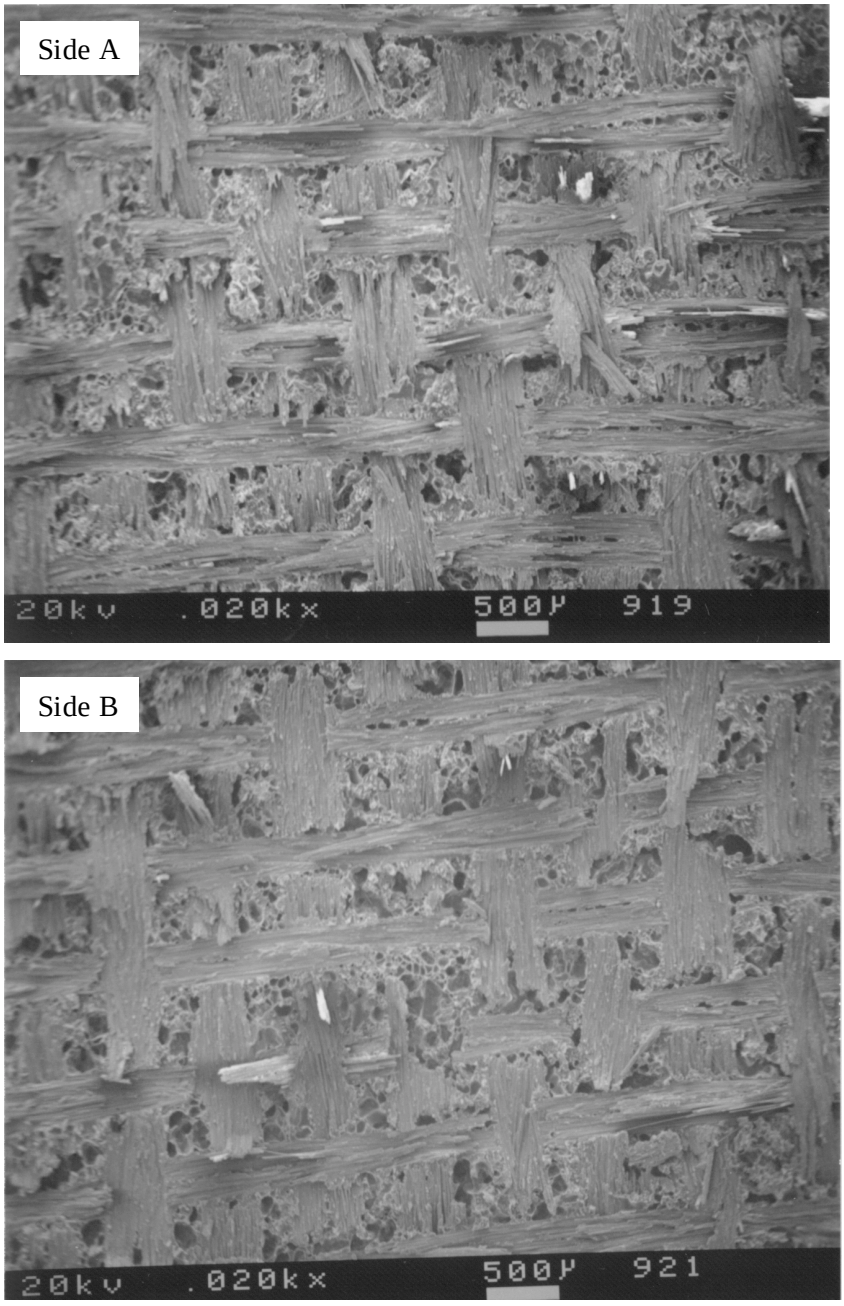

Figure 4.53. SEM photomicrographs of failure surfaces of a representative wedge specimen that was bonded and then thermally treated at 371°C for 1.0 hour in air (bond/heat) and immersed in boiling water for 144 hrs. The SEM photomicrographs of the two failure surfaces are not necessarily for corresponding spots.

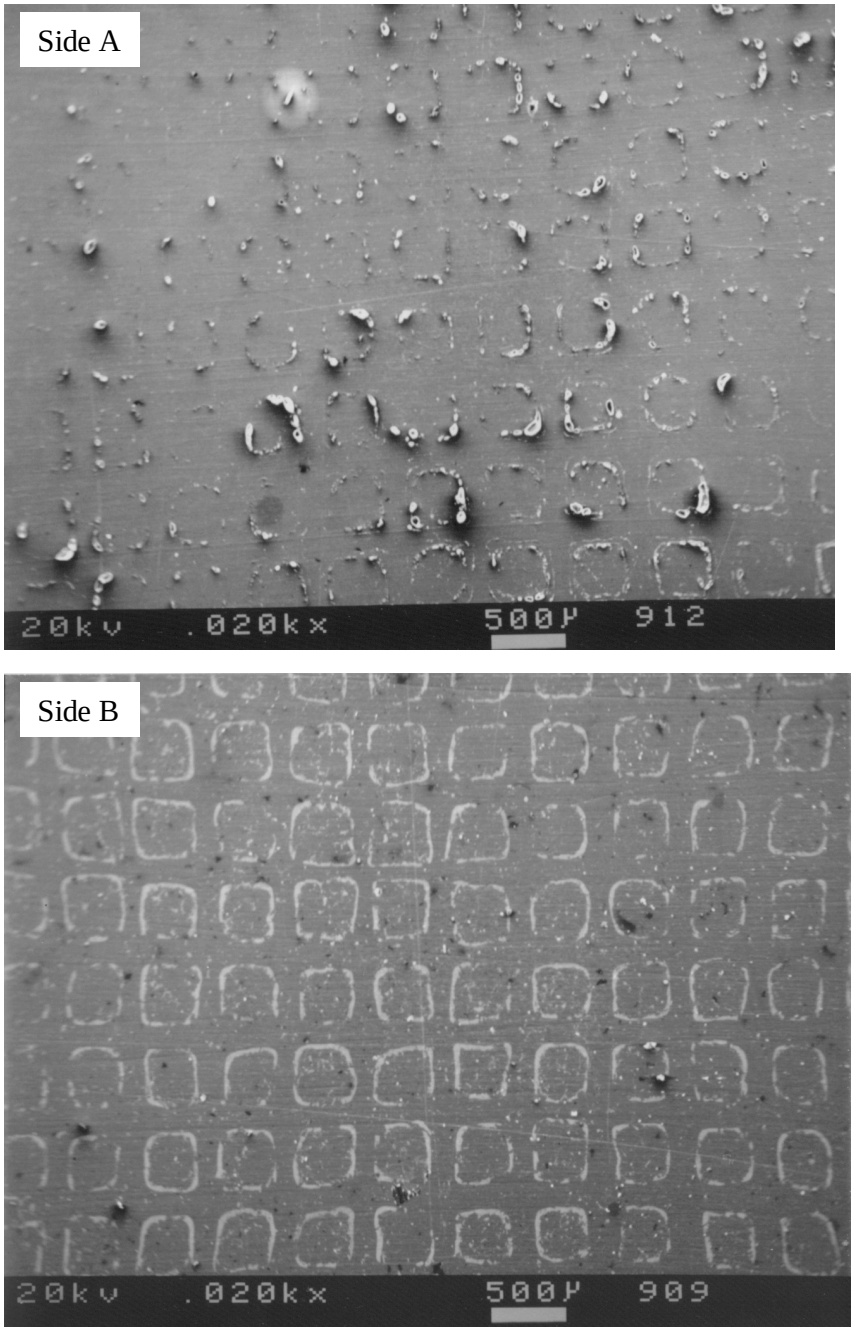

Figure 4.54. SEM photomicrographs of failure surfaces of a representative wedge specimen that was bonded and then thermally treated at 371°C for 3.0 hours in air (bond/heat) and immersed in boiling water for 144 hrs. The SEM photomicrographs of the two failure surfaces are not necessarily for corresponding spots.

4.3.2.3 Surface Characterization of Failure Surfaces by Diffuse Reflectance FTIR

Figure 4.55 shows the diffuse reflectance spectra for failure surfaces (side A and side B) for wedge specimens that were prepared by a thermal treatment at 371°C for 0.5 and 3.0 hrs, bonded (heat/bond) and then immersed in boiling water for 144 hours. The spectra for failure surfaces for as-bonded (non-treated) and for wedge specimens that had been bonded and then thermally treated (bond/heat) at 371°C for 0.5 and 1.0 hours and then immersed in boiling water for 144 hours are shown in Figure 4.56. The spectra for the two failure sides (side A and side B) for as-bonded (no thermal treatment), heat/bond and bond/heat wedge specimens are similar to that of diffuse reflectance FTIR spectrum for cured FM-5 adhesive (see Figure 4.7). No detectable chemical degradation of the FM-5 adhesive resin via hydrolysis (upon exposure to boiling water) has occurred (the characteristic polyamic absorption band at about 3300 cm^{-1} corresponding to N-H stretching was not observed), all characteristic polyimide absorption bands at 1778 cm^{-1}, 1730 cm^{-1}, 1378 cm^{-1}, 1104 cm^{-1} and 740 cm^{-1} were observed in the FTIR spectrum.

Figure 4.57 shows the diffuse reflectance FTIR spectra for the two failure surfaces (side A and side B) for bond/heat wedge specimens that were prepared by thermal treatment at 371°C for 3 hours. This specimen failed upon wedge insertion and therefore was not immersed in boiling water. The FTIR spectrum of the side A failure surface shows all the characteristic imide bands of cured FM-5 adhesive. Even though side A has an oxide coating on top of the adhesive (determined from XPS analysis), a relatively greater sampling depth of about 1-3 μm in the FTIR method of analysis allows obtaining a diffuse reflectance spectrum of subsurface bulk adhesive. The FTIR spectrum of the side B failure surface, however, does not show any characteristic imide bands; instead, the spectrum resembles the diffuse reflectance FTIR spectrum of an as-anodized non-bonded Ti-alloy surface. A broad absorption peak in the range 1100 to 1300 cm-1 observed in FTIR spectrum of the side B surface was also observed in the spectrum for CAA Ti-6Al-4V alloy surface.

4.3.2.4 XPS Surface Analysis of Failure Surfaces

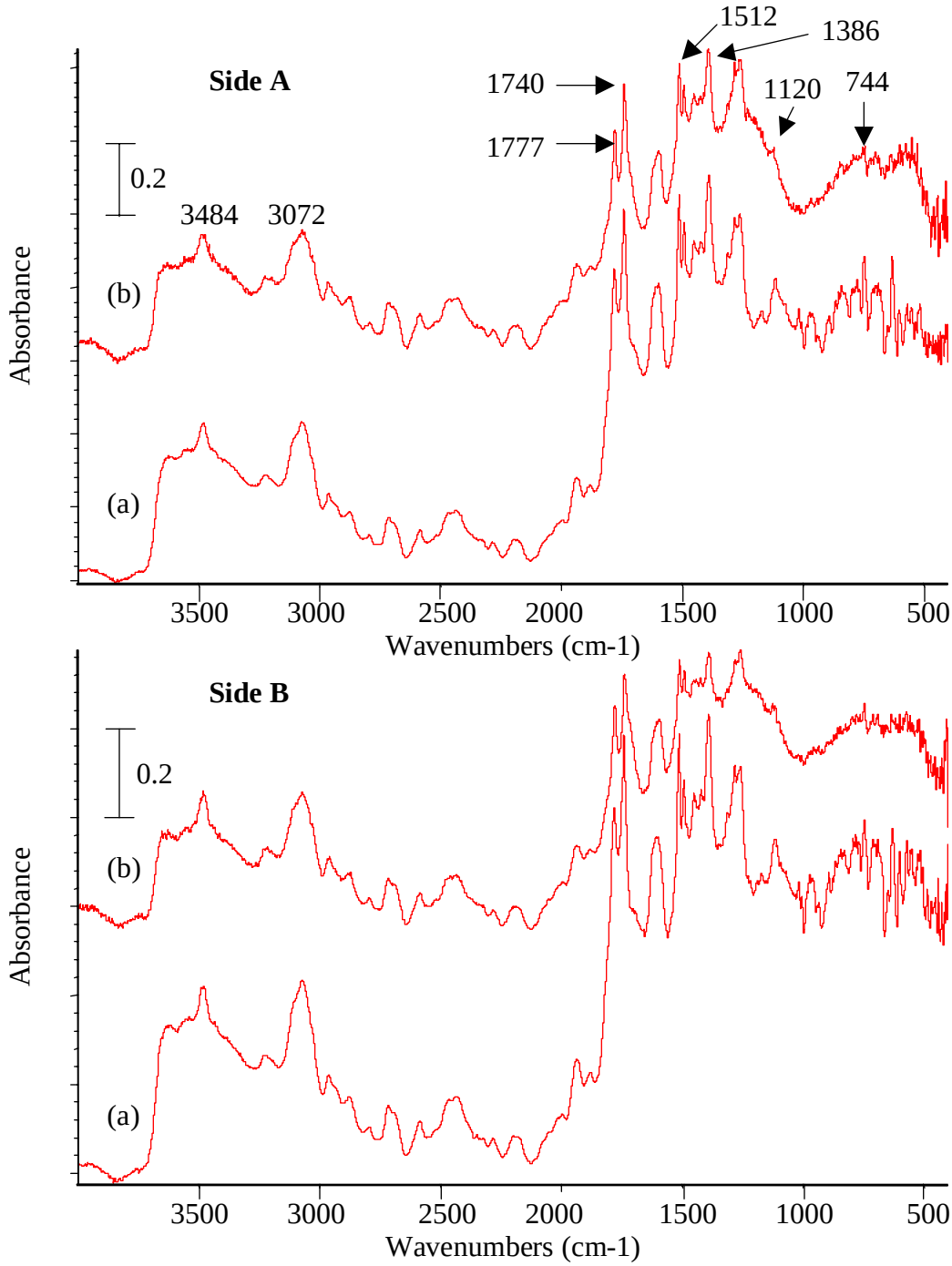

Figure 4.55. The diffuse reflectance FTIR spectra of side A and side B failure surfaces for heat/bond wedge specimens that were thermally treated at 371°C for (a) 0.5 hr and (b) 3.0 hrs and then immersed in boiling water for 144 hrs.

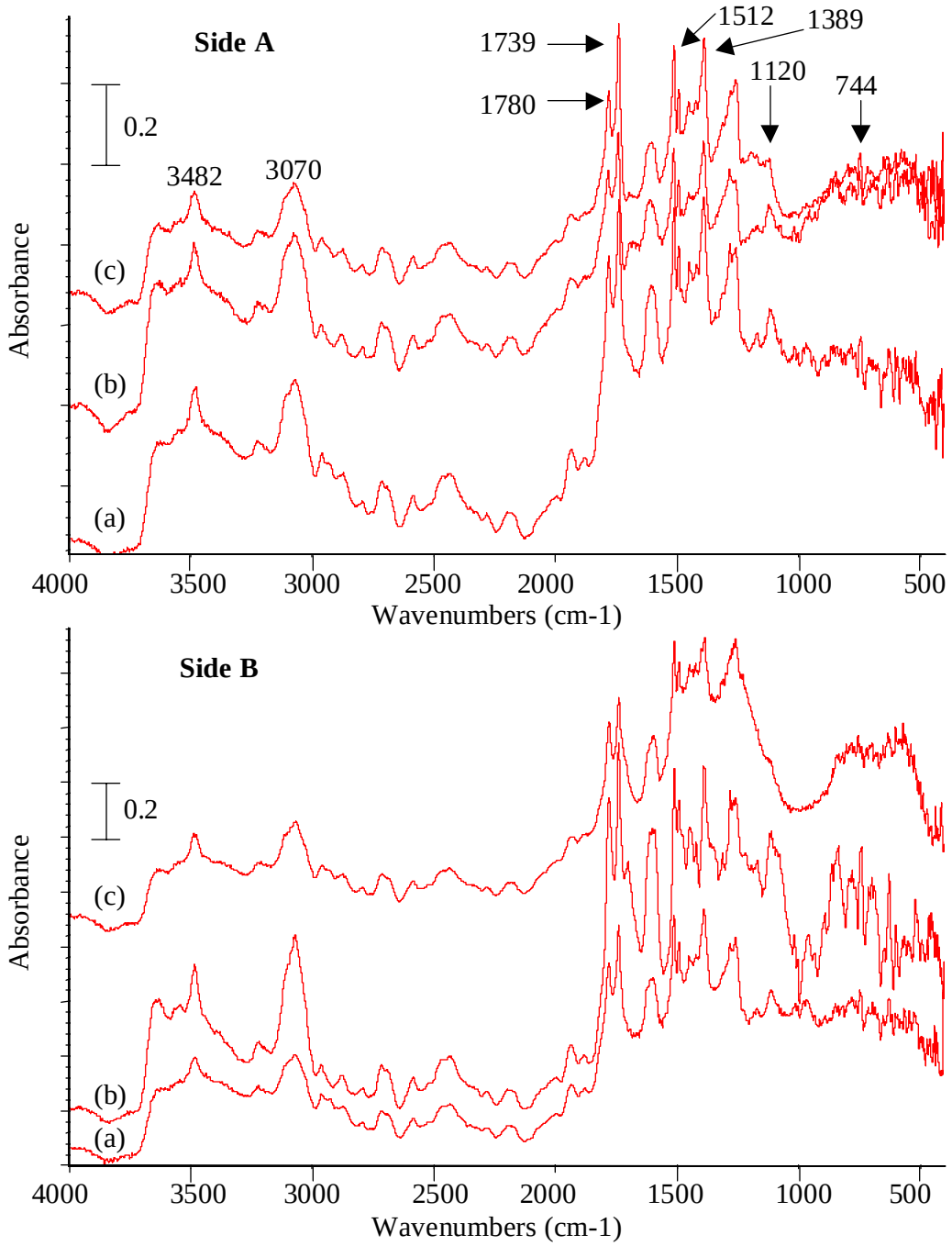

Figure 4.56. The diffuse reflectance FTIR spectra of side A and side B failure surfaces for (a) non-treated wedge specimen and for bond/heat wedge specimens that were thermally treated at 371°C for (b) 0.5 hr and (c) 1.0 hr and then immersed in boiling water for 144 hrs.

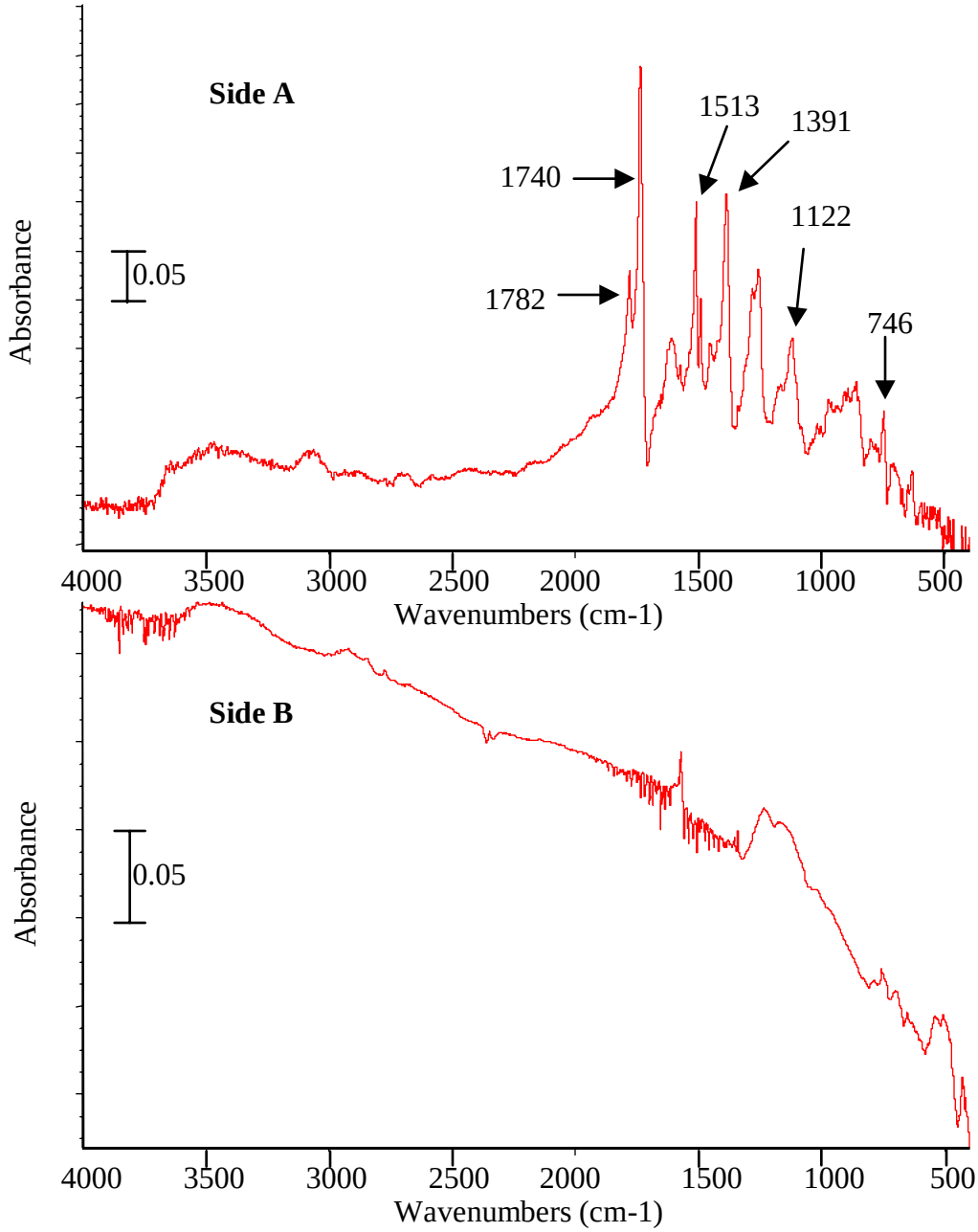

Figure 4.57. The diffuse reflectance FTIR spectra of side A and side B failure surfaces for bond/heat wedge specimen that was thermally treated at 371°C for 3.0 hours in air.

The XPS results for failure surfaces of as-bonded specimens (no heat treatment) are presented in Table 4.23. The two failure surfaces are arbitrarily labeled side A and side B. The XPS surface analysis of the two failure surfaces were not necessarily carried out on corresponding spots. These results support the SEM findings, and revealed that the two failure surfaces (side A and side B) are chemically equivalent. The XPS analysis of failure surfaces shows that the atomic concentrations for carbon, oxygen, nitrogen, and silicon are typical of the values anticipated for failure surfaces produced via debonding within the scrim cloth of the supported FM-5 adhesive. The atomic concentrations of carbon, oxygen, nitrogen and silicon on each failure surface are typical of the bulk composition of cured FM-5 adhesive. The elements titanium, fluorine and calcium were present in very small amounts (≤ 0.2 atomic %) and aluminum was detected (~ 1.0 at.%) on each failure surface. However, the source of aluminum could not have been from the CAA oxide because titanium, which is a major component of the alloy and oxide, was not detected (≤ 0.2 atomic %) on the failure surfaces. The aluminum could have been deposited on failure surfaces from aluminum contaminated boiling water. One possible source of aluminum contamination in boiling water could be the alloy (Ti-6Al-4V) from the bonded specimen itself.

The relevant XPS results for failure surfaces for heat/bond specimens are summarized in Table 4.24, and support the SEM findings, viz., that the failure is cohesive in the adhesive. The results further revealed that the two failure surfaces (side A and side B) are chemically equivalent for samples that were heated at 371°C for 0.5, 1.0 and 3.0 hours and then bonded. For a failure that is cohesive in the adhesive, the two sides are equivalent and can be arbitrarily labeled A and B. The analysis results indicate that failure occurred within the adhesive. This conclusion is supported by the fact that no titanium is detected (<0.2 at.%) on either failure surface for samples prepared using either treatment. As discussed earlier, the presence of aluminum (0.6 to 2.0 at.%) on each failure surface is possibly from aluminum removed from the test specimen during the boiling water test. Silicon from the scrim cloth is also detected on each failure surface at a level that is typical of specimens that fail at the scrim cloth-adhesive interface. Further, calcium is also detected on each failure surface. The most likely source of calcium is from the

Table 4.23. The surface atomic concentrations of elements, as determined by XPS analysis of failure surfaces of as-bonded chromic acid anodized Ti-6Al-4V specimens (non-treated) immersed in de-ionized water for about 144 hours. Standard deviations are given at the 95% confidence limit.

Element	Side A	Side B
C	73.9 ± 1.6	73.5 ± 1.6
O	19.1 ± 1.3	19.5 ± 1.6
N	4.0 ± 0.1	3.6 ± 0.3
Si	2.1 ± 0.3	2.3 ± 0.4
Ti	< 0.2	< 0.2
Al	0.9 ± 0.2	1.1 ± 0.2
F	< 0.2	< 0.2
Ca	< 0.2	< 0.2

Table 4.24. The surface atomic concentrations of elements, as determined by XPS analysis of failure surfaces of wedge specimens that were prepared by a thermal treatment at 371°C in air for 0.5, 1.0 and 3.0 hours, bonded (**heat/bond** specimens) and then immersed in boiling water for about 144 hrs. Standard deviations are given at the 95% confidence limit.

Element	0.5 hour		1.0 hour		3.0 hours	
	Side A	Side B	Side A	Side B	Side A	Side B
C	64.3 ± 3.2	65.7 ± 1.4	67.5 ± 3.8	69.2 ± 4.1	74.0 ± 2.9	73.1 ± 3.0
O	24.7 ± 2.2	23.6 ± 1.4	22.1 ± 2.8	21.0 ± 2.7	18.2 ± 1.3	18.6 ± 1.5
N	4.0 ± 0.3	4.2 ± 0.4	3.8 ± 0.6	3.5 ± 0.2	4.7 ± 0.3	5.0 ± 0.2
Si	4.1 ± 0.3	3.6 ± 0.2	3.7 ± 0.8	3.4 ± 1.0	2.1 ± 0.2	2.3 ± 0.5
Ti	< 0.2	< 0.2	< 0.2	< 0.2	< 0.2	< 0.2
Al	1.7 ± 0.3	2.0 ± 0.5	1.4 ± 0.5	1.5 ± 0.5	0.6 ± 0.2	0.6 ± 0.2
F	< 0.2	< 0.2	< 0.2	< 0.2	< 0.2	< 0.2
Ca	1.2 ± 0.3	0.9 ± 0.2	1.5 ± 0.2	1.4 ± 0.1	0.4 ± 0.6	0.4 ± 0.4

scrim cloth or from boiling water. The XPS surface analysis of as received neat scrim cloth (without any adhesive coatings on it) revealed that calcium is one of the components on the scrim cloth surface. In addition, the shape of the carbon 1s photopeak is indicative of polyimide adhesive, for example, see Figure 4.58. The XPS results demonstrate that failure occurred at the scrim cloth-adhesive interface.

The relevant XPS results for failure surfaces for bond/heat specimens are summarized in Table 4.25. The results support the SEM findings and illustrate the differences in failure modes when comparing the results for **heat/bond** specimens with data for **bond/heat** samples. For a failure in the oxide, the side that has an oxide coating is indicated as side A. The other failure side (surface with a very thin coating of oxide on the surface) is designated as side B. The XPS results revealed that the two failure surfaces (A and B) are chemically equivalent for samples that were bonded and heated at 371°C for 0.5 and 1.0 hours, and that failure occurred within the adhesive. This conclusion is supported by the fact that no titanium is detected (<0.2 at.%) on either failure surface. Further, silicon from the scrim cloth is also detected on each failure surface at a level that is typical of that noted for specimens that fail at the scrim cloth-adhesive interface. The element calcium was also detected on each failure surface. As discussed before, the most likely source of calcium is from the scrim cloth or from the boiling water. The shape of the carbon 1s photopeak is indicative of polyimide adhesive, for example, see Figure 4.59. The XPS results demonstrate that failure occurred at the scrim cloth-adhesive interface.

Surface analysis results are also given in Table 4.25 for a sample that was bonded and then thermally treated at 371°C in air for 3 hours. The important results are that significant concentrations of titanium are detected on each failure surface, fluorine and aluminum are noted, nitrogen is at a low concentration, and silicon is not detected. It is also observed that the concentrations of aluminum and fluorine are greater on side A than on side B. That equivalent concentrations of titanium, little nitrogen, and no silicon are detected on each failure surface, indicates failure within the anodic oxide layer. The presence of adhesive as well as fluorine in

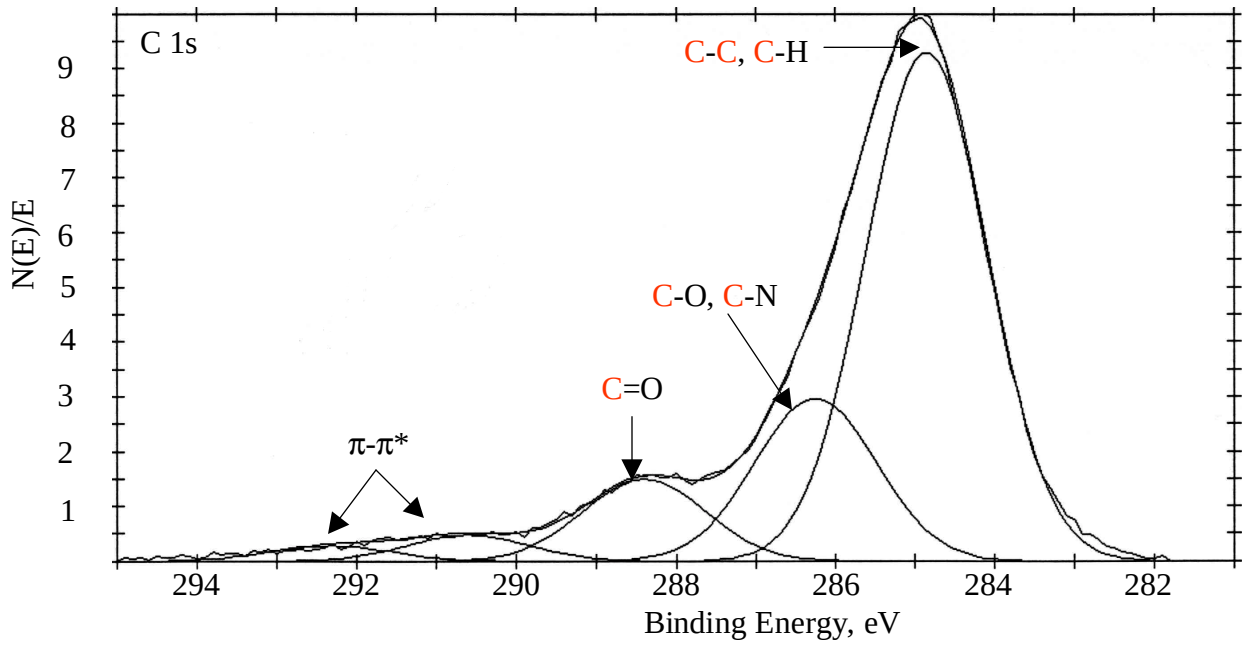

Figure 4.58. The carbon (C 1s) XPS photopeak for Side A failure surface for heat/bond wedge specimen that was thermally treated at 371°C for 1 hour in air and then immersed in boiling water for 144 hrs.

Table 4.25. The surface atomic concentrations of elements, as determined by XPS analysis of failure surfaces of wedge specimens that were bonded and then thermally treated (**bond/heat** specimens) at 371°C in air for 0.5, 1.0 and 3.0 hours and then immersed in boiling water for about 144 hours. Standard deviations are given at 95% confidence limit.

Element	0.5 hour		1.0 hour		3.0 hours	
	Side A	Side B	Side A	Side B	Side A	Side B
C	73.3 ± 1.1	73.1 ± 1.5	71.7 ± 3.1	73.6 ± 1.6	17.2 ± 1.6	33.9 ± 1.2
O	20.8 ± 0.4	20.9 ± 1.2	20.4 ± 3.0	18.2 ± 0.6	38.5 ± 1.8	44.0 ± 0.9
N	3.9 ± 0.3	4.5 ± 0.1	4.1 ± 0	3.7 ± 0.3	1.0 ± 0.1	0.8 ± 0
Si	1.7 ± 0.3	1.5 ± 0.4	3.1 ± 0.7	2.7 ± 0.5	< 0.2	< 0.2
Ti	< 0.2	< 0.2	< 0.2	< 0.2	14.0 ± 1.2	15.8 ± 0.2
Al	< 0.3	< 0.3	< 0.3	1.0 ± 0.1	7.1 ± 0.6	2.8 ± 0.2
F	< 0.2	< 0.2	< 0.2	< 0.2	22.2 ± 1.7	2.7 ± 0.1
Ca	< 0.2	< 0.2	0.7 ± 0.6	0.8 ± 0.1	< 0.2	< 0.2

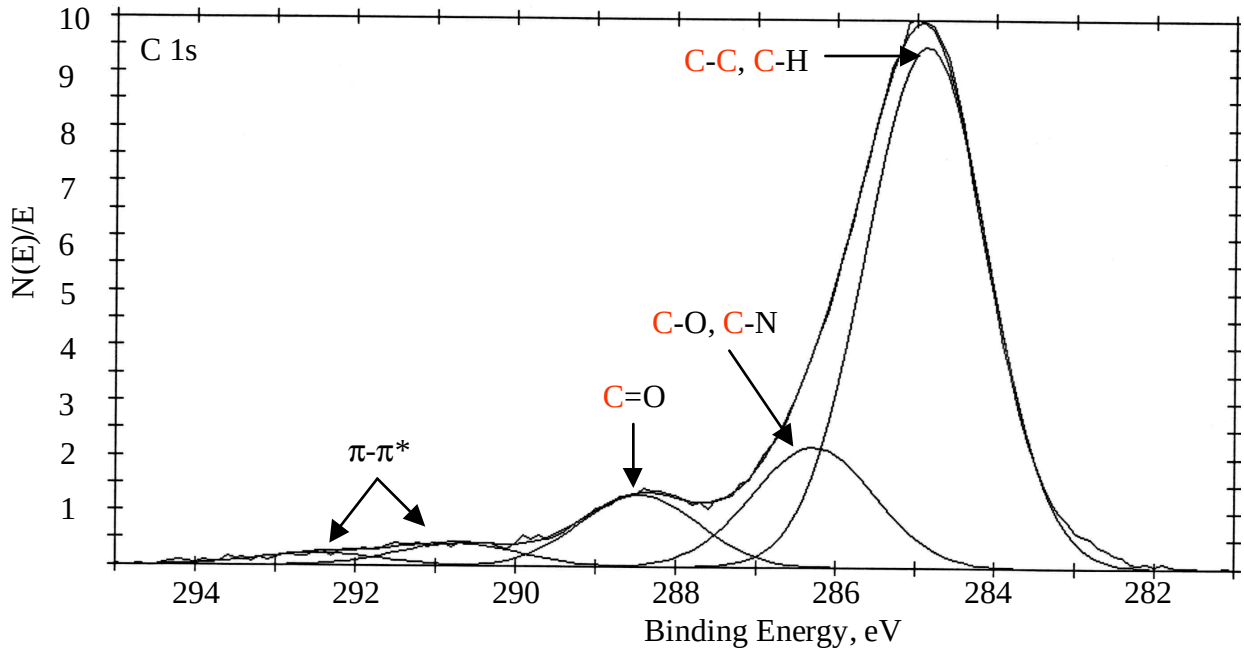

Figure 4.59. The carbon (C 1s) XPS photopeak for Side A failure surface for bond/heat wedge specimen that was thermally treated at 371°C for 1 hour in air and then immersed in boiling water for 144 hrs.

the oxide coating on both failure surfaces suggests that the locus of failure is not at the oxide/metal interface. The significant relative amounts of fluorine and aluminum on failure surface A suggest that these elements, or compounds containing these elements, are associated with the anodic oxide degradation process and contribute to failure in the durability tests.

The AES characterization results also suggest that failure takes place within the anodic oxide coating, primarily near the oxide/metal interface. The AES sputter depth profile results (atomic concentration versus sputter time) of failure surfaces of the bond/heat (371°C/3 hrs/air)-wedge specimen are shown in Figure 4.60. The AES sputter-depth profile of side A indicates a relatively thick oxide coating on the adhesive film. However, the oxide/adhesive interface is not sharp. The presence of carbon in the oxide layer indicates good wetting of the porous oxide by the adhesive film during the bonding process. The AES sputter-depth profile indicates a relatively thin oxide layer on the metal side (side B) of the failure surface.

The curve fit XPS spectra in the aluminum 2p and fluorine 1s regions for an as-anodized titanium alloy surface and for the "A" side surface of the failed bond/heat sample (371°C for 3 hours) are presented in Figures 4.61 and 4.62, respectively. The respective Al 2p and F 1s spectra for the as anodized, non-treated specimen exhibit only one photopeak. The binding energy for aluminum suggests the presence of an aluminum oxide or hydrated oxide, while the binding energy for fluorine indicates adsorbed fluoride ion.

The aluminum 2p and fluorine 1s photopeaks from XPS analysis of the failure surfaces (side A) for bond/heat samples could each be resolved into two components. Each new component occurs at a higher binding energy than that for aluminum oxide or adsorbed fluorine. The binding energies for aluminum and fluorine as fluoride from the curve fit data were 76.1 eV and 686.7 eV, respectively. These values are in close agreement with those reported for aluminum and fluorine in AlF_3 [207, 208]. Based on binding energy data for AlF_3, the high binding energy peak for aluminum is assigned to aluminum fluoride. The high binding energy peak for fluorine is attributed to fluorine in aluminum fluoride.

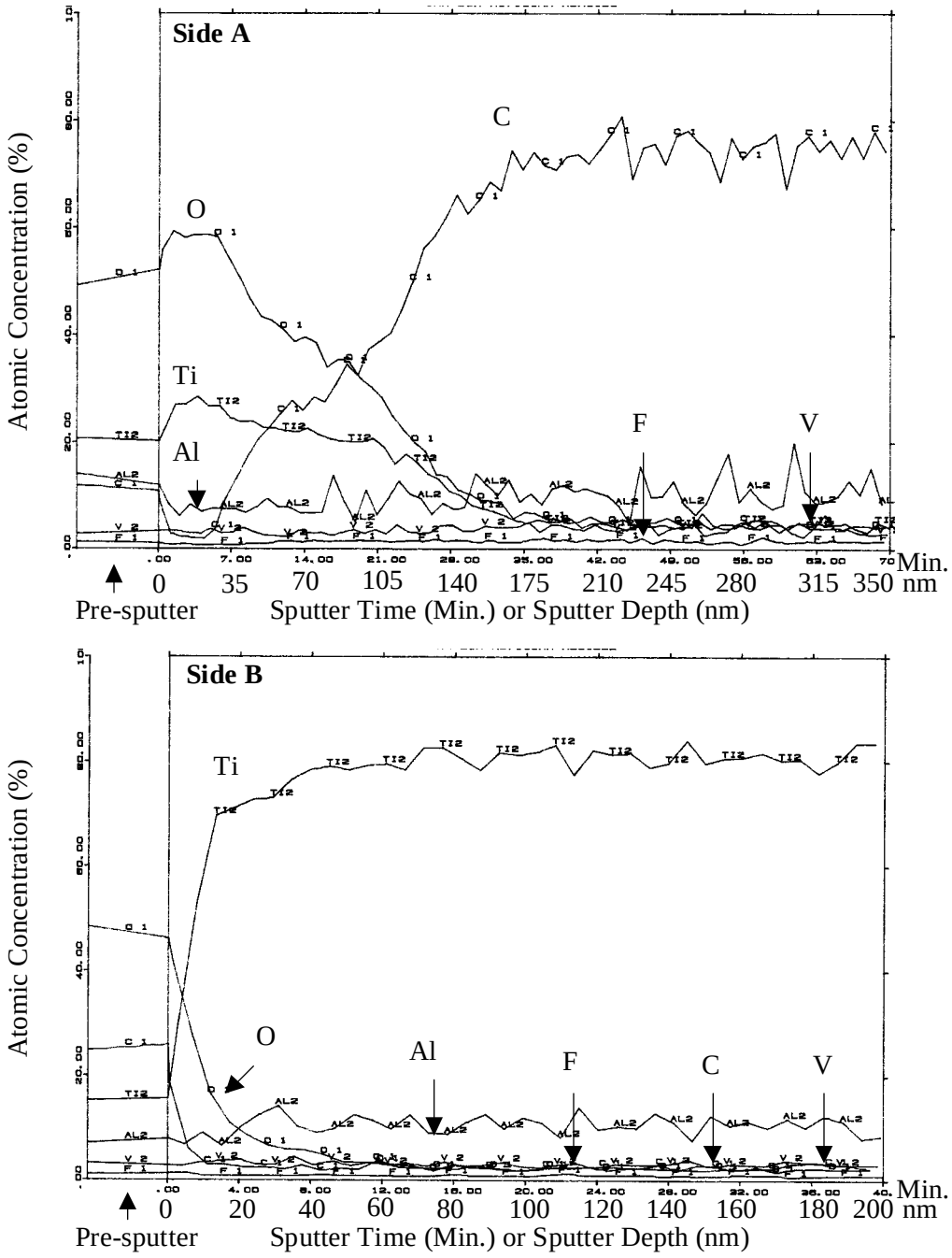

Figure 4.60. Auger sputter-depth profiles for the failure surfaces of bond/heat (371°C/3.0 hrs/air)-wedge specimen: (a) Side A and (b) Side B.

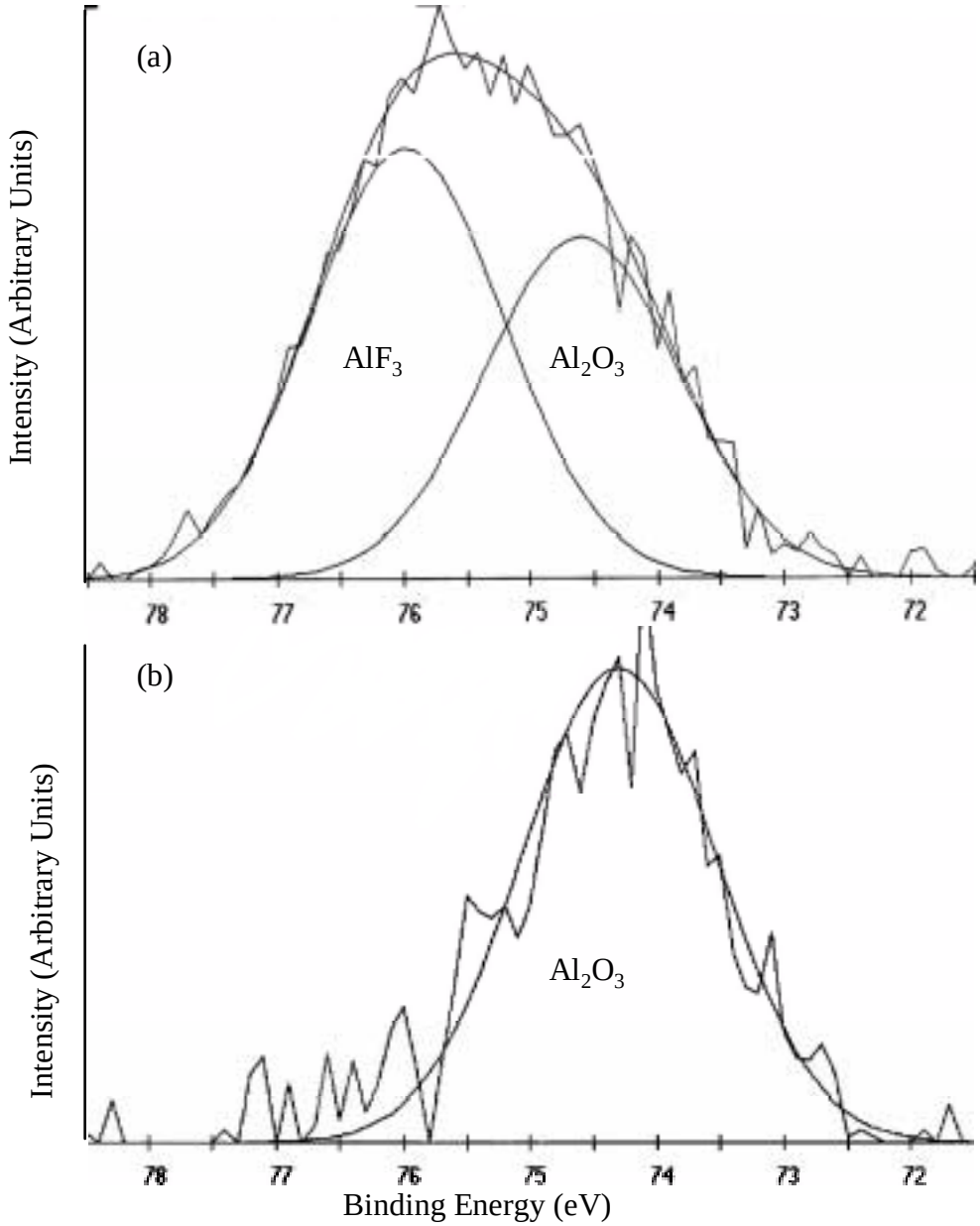

Figure 4.61. The curve fit XPS spectra in the aluminum 2p region for (a) the "A" side surface of the failed bond/heat sample (371°C for 3 hours), and for (b) an as-anodized titanium alloy surface.

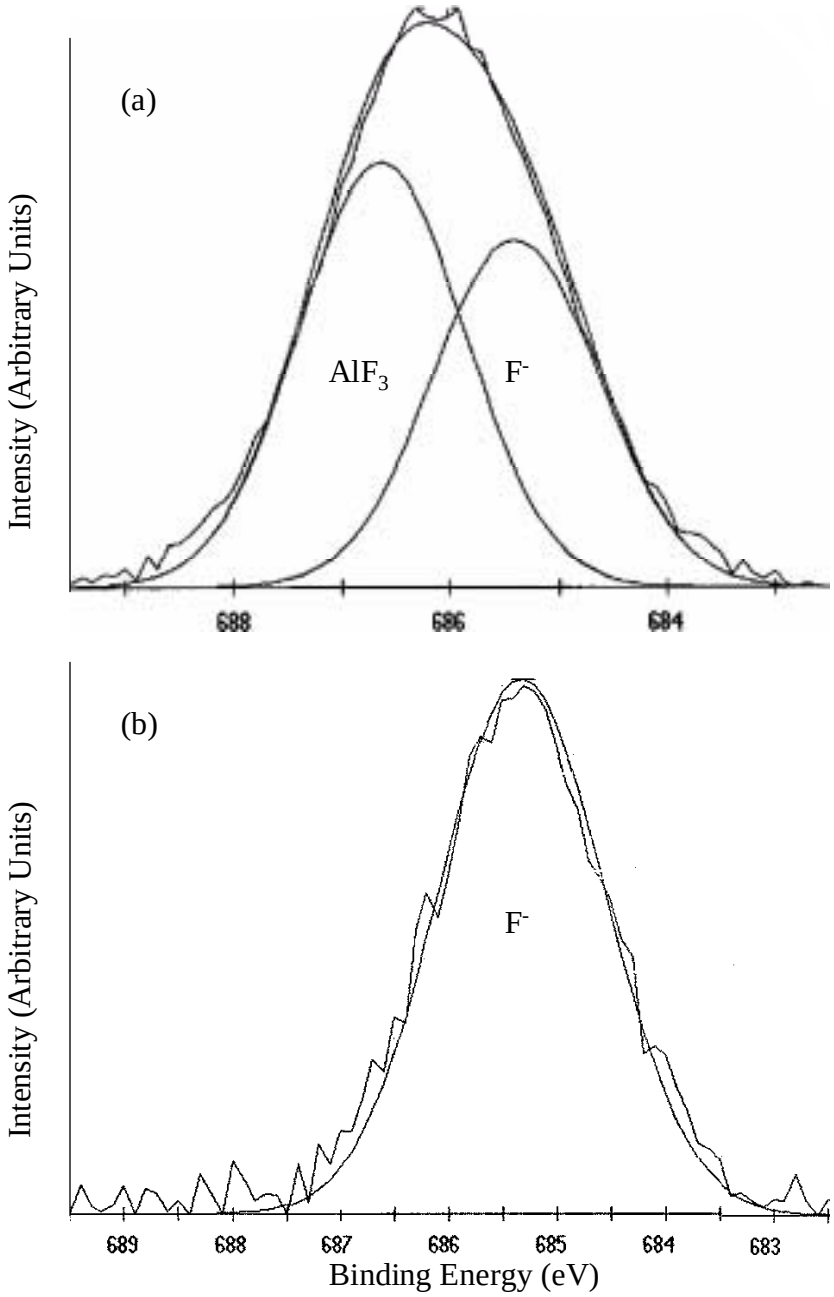

Figure 4.62. The curve fit XPS spectra in the fluorine 1s regions for (a) the "A" side surface of the failed bond/heat sample (371°C for 3 hours), and for (b) an as-anodized titanium alloy surface.

Using the atomic percentages for the aluminum – fluorine components in the Al 2p and F 1s peak envelopes, an approximate empirical formula for an aluminum – fluorine compound was determined. From XPS curve-fit analysis of the "A" oxide-failure regions of bond/heat specimens, the fluorine-to-aluminum ratio ranged between 2.9 and 4.0, with an average ratio of 3.4. The ratio closely agrees with that for an aluminum fluoride (AlF_3) composition. The higher F/Al ratios (F/Al > 3.0) on some failure surfaces may be due to aluminum fluoride complexes of the form $[AlF_n^{3-n}]$ in combination with some aluminum oxy-fluoride $[Al(OF)_n^{3-3n}]$ compounds.

Fluoride ion in the anodic oxide coating of the titanium alloy could react with metal compounds and/or metals at the oxide/alloy interface to form metal fluorides. Based on the evidence obtained from XPS analysis of failure specimens, it is apparent that only aluminum reacted with fluoride to form aluminum fluoride. The two possible reactions for the formation of aluminum fluoride are given below:

$Al_2O_3(s) + 6HF(g) \rightarrow 2AlF_3(s) + 3H_2O(l)$, ΔG^0 (reaction at 25°C) = -343.6 kJ.....(1)

$3Al(s) + 6HF(g) \rightarrow 2AlF_3(s) + 3H_2(g)$, ΔG^0 (reaction at 25°C) = -1214.6 kJ ---------- (2)

Aluminum oxide and hydrofluoric acid in the CAA oxide could react to produce aluminum fluoride during the thermal treatment following bonding, and aluminum metal at the oxide/alloy interface and hydrofluoric acid could react to produce aluminum fluoride. ΔG^0 for the above reactions at 25°C are –343.4 kJ and -1214.6 kJ as calculated from literature data [137-139]. The negative ΔG^0 value for the reactions suggest that the above processes are at least thermodynamically favorable at 25°C. The above reactions are thermodynamically favorable also at 427°C (see Table 2.1). The fact that the failure in the oxide coating occurred very close to the oxide/alloy interface suggests that both aluminum oxide and aluminum metal react with hydrofluoric acid to produce aluminum fluoride.

In a series of investigations by Clearfield et al. [7, 8], CAA titanium alloy was subjected to thermal treatment at 330°C for 160 and 2000 hours in air. CAA titanium alloy was also exposed to higher treatment temperatures, 400°C for 24 hrs and 450°C for 3 hrs and 24 hrs, but the thermal treatment was carried out in vacuum. The locus of failure was in the oxide for a CAA specimen that was thermally treated in vacuum at 400°C and 450°C. The CAA titanium specimen thermally treated in vacuum at 330°C in air failed via mixed mode when treated for 160 hrs, whereas failure was in the oxide coating when treated for 2000 hours. Clearfield et al. observed a significant tailing of the oxygen signal (metal/oxide interface was not sharp) in an AES depth profile for a thermally-treated (in vacuum) CAA Ti-6Al-4V alloy. The oxygen concentration immediately below the surface was near the solubility limit (about 25 at.%) in the alloy. Clearfield and associates suggested that at temperature approaching 300°C oxide dissolution takes place. The dissolution of oxygen results in the formation of non-stoichiometric oxides and an embrittled region below the oxide. These regions could weaken the oxide of the interphase and cause bond failure.

In the wedge specimens, it could be anticipated (based on the work of Clearfield et al.) that oxygen dissolution would be dissimilar in a non-bonded CAA titanium alloy compared with a bonded specimen, since the CAA titanium alloy surface in the former is comparatively less protected from the oxidizing environment. If oxygen dissolution plays a significant role in causing bonds to fail at the oxide/metal interface, then the heat/bond wedge specimen should have failed in the oxide coatings. XPS results for thermally-treated (371°C for 3.0 hrs) wedge specimens indicate bond failure in the adhesive for the heat/bond specimen and in the oxide for the bond/heat specimen. It does not appear that this difference in the failure modes for **heat/bond** and **bond/heat** specimens could be explained on the basis of an oxygen-dissolution mechanism.

The differences in the failure mode when comparing the **bond/heat** and **heat/bond** is attributed to the formation of an aluminum fluoride. The basic difference between the two treatments (**heat/bond** and **bond/heat**) is in the chemical composition of their respective anodic oxides.

Fluorine is not detected in the CAA oxide when a CAA Ti-6Al-4V alloy (non-bonded) is thermally treated at 371°C for 3.0 hours in air, see Table 4.14. The XPS depth profile data clearly show the absence of fluorine in the anodic oxide. A plausible explanation is that a fluorine-containing compound, perhaps HF, in the oxide is removed via desorption. On the other hand, when CAA titanium alloy is bonded prior to any thermal treatment, fluoride ions are trapped within the oxide by the adhesive film during the bonding process. Thus, when a CAA titanium alloy is bonded and then thermally treated at high temperatures (>350°C), the fluoride ions in the oxide react with aluminum to form aluminum fluoride species.

Although the reaction between aluminum oxide and hydrofluoric acid is thermodynamically favorable at room temperature, the reaction does not take place at any noticeable rate at room temperature. Therefore, it is not surprising that industrial production of aluminum fluoride is carried out by a dry process, where Al_2O_3 is treated at 550°C to 600°C in a continuous stream of gaseous hydrofluoric acid [140].

On the other hand, the absence of fluoride ions in the oxide for a **heat/bond** specimen does not facilitate the formation of aluminum fluoride species and thus, there is no weakening of the anodic oxide coatings. However, it must also be pointed out that the **bond/heat** wedge specimen that is thermally treated at 371°C for 1.0 hour in air, does not fail in the oxide coating. The absence of failure in the oxide could be due to the fact that an insufficient quantity of aluminum fluoride has formed to cause oxide failure under the given mechanical load (wedge) condition. It is known from single-lap test results (see Table 4.30) that thermally-treated lap specimens increasingly fail in the oxide coating (increasingly more aluminum fluoride is formed) as the temperature and duration of the thermal treatment are increased.

Based on the surface analysis results and thermodynamic considerations, it is reasoned that oxide failure in the durability tests is due to the formation of an aluminum fluoride which destroys the integrity of the CAA anodic oxide. The degradation occurs in the bonded specimens during the various “bond/heat” thermal treatments.

A number of reasons for the weakening of the oxide film could be suggested, but three possibilities merit discussion: (1) The formation of aluminum fluoride species as a result of reaction between hydrofluoric acid and aluminum oxide, introduces large compressive stresses in the oxide due to an increase in the oxide volume. The densities of titanium oxide (TiO_2), aluminum oxide (Al_2O_3) and aluminum fluoride (AlF_3) are 4.24 g/cm^3, 3.965 g/cm^3 and 2.882 g/cm^3, respectively [209, 210]. The presence of compressive stresses in the oxide could result in cracking and spalling of the oxide coating under minimal load (mechanically weak oxide film). (2) The fluoride ions could react directly with the metal at the oxide/metal interface to form products at the interface, which could lead to weakening or even debonding of the oxide from the metal (e.g., $2Al + 6HF = 2AlF_3 + 3H_2$). (3) Any significant differences in the coefficients of thermal expansion (CTE) between oxides and fluorides could result in a stress build-up inside the oxide when the test sample is cooled after the thermal treatment. Such stresses could promote failure in the oxide.

4.4 Lap Shear Test Results

4.4.1 Non-thermally Treated Specimens

The average lap-shear strength for as-bonded (non-treated) specimen is 49.5 ± 1.5 MPa (7183 psi). The SEM photomicrographs of failure surfaces for non-thermally treated lap specimens are shown in Figure 4.63. The SEMs in Figure 4.63 show the two different sides of the same sample. Since the failure (visually) was entirely within the adhesive, the two failure surfaces from the same lap specimen were arbitrarily labeled as Side A and Side B. The weave-type features in the SEM photomicrographs are characteristic of the pattern of the woven glass scrim cloth in the adhesive. Since the weave-type pattern is observed on each failure surface, the SEM photomicrographs suggest that failure occurred within the adhesive.

The XPS results for failure surfaces for non-treated lap specimens are summarized in Table 4.26. The XPS results support the SEM findings. The atomic concentrations for carbon, oxygen,